GLOBAL MODES CONSTITUTING THE SOLAR MAGNETIC CYCLE

I. *Search for 'Dispersion Relations'*

M. H. GOKHALE, J. JAVARAIAH, K. NARAYANAN KUTTY, and B. A. VARGHESE

Indian Institute of Astrophysics, Bangalore 560034, India

(Received 18 July, 1991)

Abstract. The spherical-harmonic-Fourier analysis of the Sun's magnetic field inferred from the Greenwich sunspot data is refined and extended to include the full length (1874–1976) of the data on the magnetic tape provided by H. Balthasar. Perspective plots and grey level diagrams of the SHF power spectra for the odd and the even degree axisymmetric modes are presented. Comparing these with spectra obtained from two simulated data sets with random redistribution within the wings in the butterfly diagrams, we conclude that there is no clear evidence for the existence of any relation between the harmonic degree and the temporal frequency of the power concentrations of the inferred field. Apart from the power 'ridge' in the narrow frequency band at $\sim 1/21.4\ y^{-1}$, and low ridges at odd multiples of this frequency, there are no other spectral features. This strongly suggests that the solar magnetic cycle consists of some global oscillations of the Sun 'forced' at a frequency $\sim 1/21.4\ y^{-1}$ and, perhaps, weak resonances at its odd harmonics. The band width of the forcing frequency seems to be much less than $1/107\ y^{-1}$. In case the global oscillations are torsional MHD, the significance of their parity and power peak is pointed out.

1. Introduction

From spherical-harmonic-Fourier (SHF) analysis of the Sun's magnetic field inferred from the Greenwich sunspot data during 1902–1954 we showed earlier (Gokhale and Javaraiah, 1990a; Gokhale, Javaraiah, and Hiremath, 1990) that the butterfly diagrams could be a consequence of the near constancy of amplitudes and phases of axisymmetric odd-degree oscillations of periods ~ 22 y in the Sun's magnetic field. The amplitude spectrum of these oscillations for degrees up to $l = 13$ was shown to be similar to that of the observed magnetic field derived by Stenflo (1988) from magnetogram data during 1960–1985.

In these papers, I and II, we give an extensive study of the global modes in the solar magnetic fields using a much refined analysis of the whole data sequence (1874–1976) on the tape provided by H. Balthasar. The SHF analysis is carried out with the highest temporal frequency resolution ($\sim 1/103\ y^{-1}$) allowed by the length of the whole sequence, over an extended area of the $v - l$ plane, viz., up to $l = 36$ and $v = 55/107\ y^{-1}$, where l is the spherical harmonic degree and v is the temporal frequency. In these papers we also compare the results of our analysis with those obtained from two simulated data sets which simulate the butterfly diagrams much more realistically than an earlier simulation (Gokhale, Javaraiah, and Hiremath, 1990).

In this first paper we examine whether the SHF power of the inferred field is concentrated along any curves indicating 'dispersion relations' between the frequencies

Solar Physics **138:** 35–47, 1992.

and the degrees of the axisymmetric harmonic modes, like the one found by Stenflo and Vogel (1986) for the even degree modes.

In Section 2 we describe the refinements in the data analysis. The first one is that we take for each spot group, the data on the first day of its observed life, and attach to it a *weight* proportional to the total life of the spot group, rather than taking the data on each day of observation of the group. The other refinement consists of a thorough separation of the data coming from successive sunspot cycles during the periods of their overlaps.

In Section 3 we produce 'perspective' plots of the SHF amplitudes with respect to l and ν, for axisymmetric modes of odd and even degrees. The plot for the odd degree modes confirms that most of the SHF power of the 'inferred' magnetic field is in the narrow frequency band giving a smooth amplitude 'ridge' along $\nu = 1/21.4\ y^{-1}$ peaking at $l = 5$, 7, and a few ridges along the odd multiples of $1/21.4\ y^{-1}$. The power maxima in the successive ridges are at successively higher values of l. But there is *no* evidence for any $\nu - l$ relation up to the attained resolution and over the $\nu - l$ range covered. The same is true in the plot for the even modes, which is low and noisy.

SHF spectra of the field inferred from the maximum observed areas of the spot groups are noiser than those of the field inferred from their 'lifespans'. We therefore confine our discussion to the field inferred from the 'lifespans'.

In an attempt to bring out any hidden $\nu - l$ relations we apply the usual image processing techniques and display in Section 4 the SHF spectra in the form of grey level diagrams. These diagrams appear to indicate a possibility that the 'peaks' in the noisy spectra of the even modes are aligned along a number of curves in the $\nu - l$ plane. One also sees an alignment somewhat similar to that indicated by the magnetogram data when the analysis is confined to the years 1955–1976 and the resolution in ν is down-graded (for the sake of comparison) to $\sim 1/32\ y^{-1}$. Alignment along a few curves might appear to exist also in the diagram for the odd modes. However, either for even degrees or for odd degrees, such curves cannot be drawn unambiguously. Moreover, similar curves can be drawn even in the grey level diagrams obtained from the two 'simulated' data sets described below. We conclude that the alignments in the image processed grey-level diagrams do not provide evidence for any $\nu - l$ relations either for the even modes or for the odd modes of the inferred magnetic field.

The SHF spectra of the simulated data sets themselves yield useful information. In these simulations, unlike in the earlier simulation, the positions and the widths of the 'wings' of the butterflies in the butterfly diagrams are *individually* simulated along with their exact *asymmetries* and *overlaps*. This is achieved by randomly redistributing the latitudes of spot groups in each wing during each year over the width of the wing. In simulation 'I' the redistributions are made according to Gaussian probability distributions with the means and the standard deviations the same as those of the real data. In simulation 'II' the redistributions are made with uniform probability density over the widths of the respective wings. Both the simulated data sets yield SHF spectra broadly similar to those of the real data. Simulation 'II' is more realistic than simulation 'I'. (The difference between the real and the simulated data sets is mainly in the *phases* of the higher degree modes, which will be discussed in Paper II to follow.)

Whatever be the physical nature of the oscillations constituting the solar magnetic cycle, the spectrum of the odd degree modes in the real data indicates (as argued in Section 5) that the cycle consists of a 'forced' oscillation at $1/21.4\ y^{-1}$ and weak resonances at the odd multiples of this frequency. We also point out that if these oscillations are torsional MHD, their parity is consistent with torsion of even parity (in a poloidal field of dipole-like parity) and their power peak indicates dominance of $l = 4$–8 in the torsion. The widths of the frequency bands at the odd multiples of $1/21.4\ y^{-1}$ indicate that the bandwidth of the forcing oscillation must be much less than $1/107\ y^{-1}$.

2. The Data and the Method of Analysis

The source of our data is the same as that in Gokhale and Javaraiah (1990a), viz., Greenwich photoheliographic data for sunspot groups during 1874–1976 as recorded on the magnetic tape kindly provided by H. Balthasar. The method of analysis is also similar. However we have now analysed the full data sequence 1874–1976, and have extended the analysis to $l = 36$ and $\nu = 55/107\ y^{-1}$. Moreover we have also made the following important refinements. We find that these refinements improve the accuracy of our results by a few percent.

2.1. Definition of the 'Inferred Magnetic Field' in Terms of the 'First Day Data'

In the present analysis we have modified the earlier definition of the sunspot occurrence probability $p(\theta, \phi, t)$ during a time interval (T_1, T_2) as

$$p(\theta, \phi, t) = \begin{cases} (n_k/N)\,\delta(\mu - \mu_k, \phi - \phi_k, \tau - \tau_k) & \text{at } (\mu_k, \phi_k, \tau_k) \\ 0 & \text{elsewhere}, \end{cases} \tag{1}$$

where θ and ϕ represent heliospheric colatitude and longitude, $\tau = (t - T_1)/(T_2 - T_1)$, t represents time measured from a suitable 'zero epoch', δ represents a delta function of its arguments, $\mu = \cos\theta$, (θ_k, ϕ_k, t_k) are the values of (θ, ϕ, t) given by the *first day's* observation of the kth spot group, n_k is the overall life span of the kth spot group, in days, and

$$N = \sum_{k=1}^{K} n_k\,, \tag{2}$$

K being the total number of all the sunspot groups observed during the interval (T_1, T_2).

In this modified definition, each spot group is considered as a phenomenon occurring at the heliospheric position where it was *first* observed. As a result, the scatter due to its subsequent proper motions gets eliminated.

Moreover, in this definition the statistical weight of a spot group is proportional to its *lifespan* rather than the number of days of its observation. Thus the statistical weights of spotgroups get *corrected for* the gaps in the observations. These corrections are particularly important for the recurrent spot groups.

Similar to the magnetic field defined in the earlier papers, the 'inferred' magnetic field

$B_{\text{inf}}(\theta, \phi, t)$ is then defined here as

$$B_{\text{inf}}(\theta, \phi, t) = \pm p(\theta, \phi, t),$$

where the sign, plus or minus, is chosen strictly according to Hale's laws of magnetic polarities of bipolar sunspot groups, taking care to separate the data from the old and the new sunspot cycles during the periods of overlaps of successive cycles (see Section 2.2).

Another measure of the 'inferred' magnetic field, $B^*_{\text{inf}}(\theta, \phi, t)$ is defined by replacing the lifespans n_k in Equation (1) and (2) by the maximum observed areas $A_{\max, k}$ of the spot groups as statistical weights of the probability distribution $p(\theta, \phi, t)$.

2.1.1. *Resulting Modifications in the Formulae for Computing SHF Amplitudes and Phases*

The definition of the inferred magnetic field in this paper has led to the following modified formulae for computing the SHF amplitudes $A(l, \nu)$ and phases $\varphi(l, \nu)$ of the axisymmetric modes in $B_{\text{inf}}(\theta, \phi, t)$ during any specified time interval (T_1, T_2) (for determining the phases of the various modes, the time interval must be at least as long as the period of oscillation):

$$A(l, \nu) = [P_c^2(l, \nu) + P_s^2(l, \nu)]^{1/2} \tag{3}$$

and

$$\varphi(l, \nu) = \tan^{-1}[P_c(l, \nu)/P_s(l, \nu)] \tag{4}$$

(to be chosen between 0° and 360° so that sin φ and cos φ have the correct signs), where

$$P_c(l, \nu) = \frac{C(l, \nu)}{N} \sum_k n_k P_l(\mu_k) \cos(2\pi \nu t_k), \tag{5a}$$

$$P_s(l, \nu) = \frac{C(l, \nu)}{N} \sum_k n_k P_l(\mu_k) \sin(2\pi \nu t_k), \tag{5b}$$

where

$$C(l, \nu) = \begin{cases} (2l+1)/2\pi, & \text{if } \nu \neq 0, \\ (2l+1)/4\pi, & \text{if } \nu = 0. \end{cases} \tag{6}$$

2.2. Separation of the Data from Successive Sunspot Cycles during the Periods of Their Overlaps

In our earlier analysis we had separated the data of successive sunspot cycles be treating the data before and after the specified dates of sunspot minima as belonging respectively to the old and the new cycles. This had caused wrong signs to be used in determining B_{inf} from the new cycle data before the dates of minima (and from the old cycle data after the dates of minima), during the few years of overlaps of the successive cycles. In the present analysis we have drawn, in the latitude-time plane, straight lines separating completely the data belonging to the old and the new cycles, and have attached appropriate signs strictly in accordance with Hale's laws of sunspot magnetic polarities.

2.3. The unit of frequency (ν_0)

The length of the full data set allows a frequency resolution $\sim 1/103\ y^{-1}$. However, from the drift rates of phases of the axisymmetric modes we have found the mean frequency of these modes to be $1/21.4\ y^{-1}$. Hence, we have taken its integral quotient nearest to $1/103\ y^{-1}$, viz., $\nu_0 = 1/107\ y^{-1}$, as the unit of frequency.

3. The SHF Amplitude Spectrum of $B_{\text{inf}}(\theta, \phi, t)$

3.1. The perspective plots

In Figure 1 we give perspective plots of the SHF amplitudes of the odd and the even degree axisymmetric modes in $B_{\text{inf}}(\theta, \phi, t)$ with respect to l and ν up to $l = 36$ and $\nu = 55\,\nu_0$.

3.2. The spectrum for the odd degree modes

It is clear that most of the SHF power is concentrated in the odd degree modes with frequencies within $\pm\,\nu_0/2$ on either side of $\nu_* = 5\,\nu_0$. (This corresponds to periods in the range 19.8 and 23.3 yr.) In this narrow frequency band the spectrum forms a smooth 'ridge' which has a 'main hump' over $l = 1$–11, with a high peak at $l = 5, 7$, and a 'tail' for $l > 19$.

There are low, 'subsidiary' ridges along $\nu = 15\,\nu_0$, $25\,\nu_0$, $35\,\nu_0$, and $44\,\nu_0$. The power concentration in the ridge along $\nu = 15\,\nu_0$ is expected in view of the asymmetry of the sunspot cycle (e.g., Bracewell, 1988). It has been shown earlier (Gokhale and Javaraiah, 1990b) that the amplitudes and phases of the modes with $\nu = 15\,\nu_0$ are correlated to those of the modes of the same l with $\nu = 5\,\nu_0$. This indicates that the secondary ridge at $\nu = 15\,\nu_0$ could be a mathematical artifact of some nonlinear dependence of the 'inferred field' on the variable representing the basic physical oscillations with $\nu_* = 5\,\nu_0$. Alternatively it could also be representing a real mode resonating at the 'third' multiple of a forcing frequency at $5\,\nu_0$, since the amplitude and phase correlations with $\nu = 5\,\nu_0$ could also result from common excitation by a single forcing oscillation. These possibilities may be true even for the other subsidiary ridges which seem to represent the set of the odd harmonics of ν_*. Thus, except for the general shift of the maximum amplitude towards larger l in the higher harmonic ridges, there is no evidence for the existence of any general $\nu - l$ relation.

3.2.1. *Spectra Obtained from the Field Inferred from Maximum Areas*

In Figure 2 we give the amplitude spectrum of the odd degree modes in the inferred field $B^*_{\text{inf}}(\theta, \phi, t)$ obtained by taking in Equation (1) statistical weights proportional to the 'maximum observed areas of sunspot groups' instead of their 'lifespans'.

It is clear that this spectrum is noisier than the one obtained from $B_{\rm inf}(\theta, \phi, t)$. Thus, the lifespan of a sunspot group gives a better measure of the associated magnetic flux than that given by the maximum observed area.

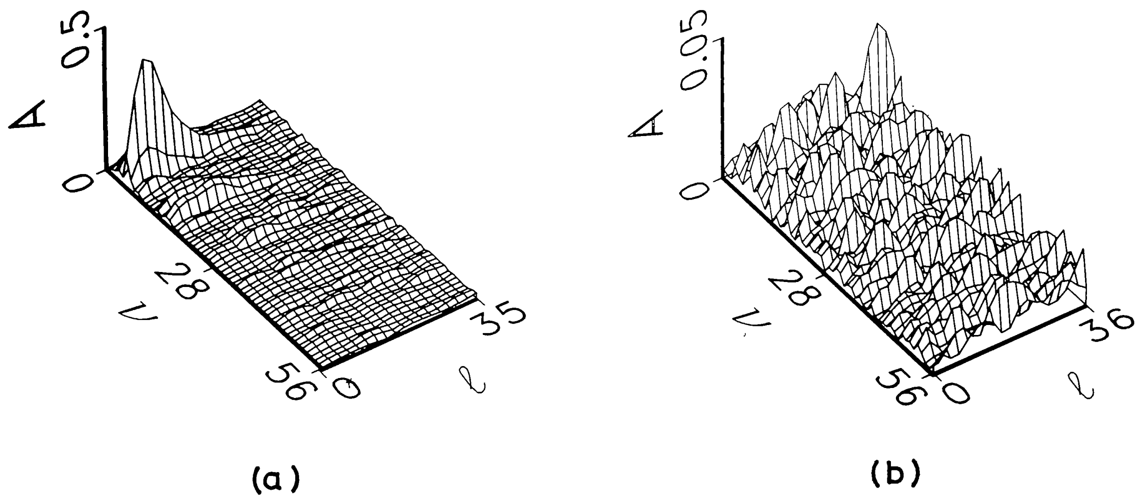

Fig. 1. Perspective plots of the SHF amplitude (A) of the axisymmetric modes of (a) odd and (b) even degree, as a function of frequency ν and degree l, in the magnetic field $B_{\rm inf}(\theta, \phi, t)$ as inferred from the sunspot data during 1874–1976 using Equation (1). The unit of frequency is $1/107\ y^{-1}$. The vertical scales of (a) and (b) are different.

3.3. The Amplitude Spectrum of the Even Degree Modes

The amplitude spectrum for the even degree modes is noisy and the level of power is comparable to that of the noise level in the spectrum for the odd modes. There is no indication of any power ridge to suggest any $\nu - l$ relation.

4. The Grey-Level Representation of the Spectra

For determining whether the local power concentrations in the SHF spectra are aligned along any curves in the $\nu - l$ plane, we made image-processed grey-level representations of the power spectra corresponding to the amplitude spectra given in Figure 1 using the standard method of hodograph equalization. These representations are shown in Figure 3(a) and 3(b). Needless to say, equal intensities do not represent equal amplitudes in these figures.

4.1. 'Apparent' Existence of $\nu - l$ Relations

These grey level representations indicate a possibility that in each of the power spectra of the odd and the even degree modes, the peaks may lie along a set of curves in the $\nu - l$ plane. One such set of curves, drawn subjectively, is illustrated in the right-hand side panel in each figure. Incidentally, these sets of curves are reminiscent of a similar looking set in the power spectra of the acoustic modes.

In particular, for comparison with the results of the analysis of the magnetogram data

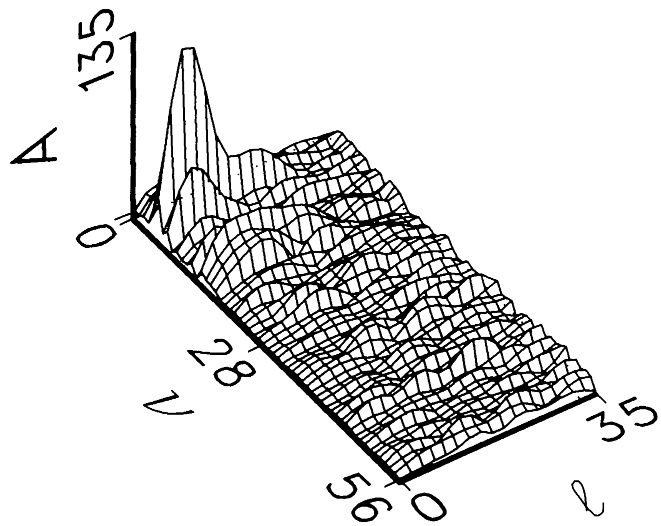

Fig. 2. Perspective plot of the SHF amplitudes of the odd degree modes given by the magnetic field obtained using 'maximum observed areas', instead of 'observed lifetimes', as statistical weights in Equation (1). Vertical unit is arbitrary.

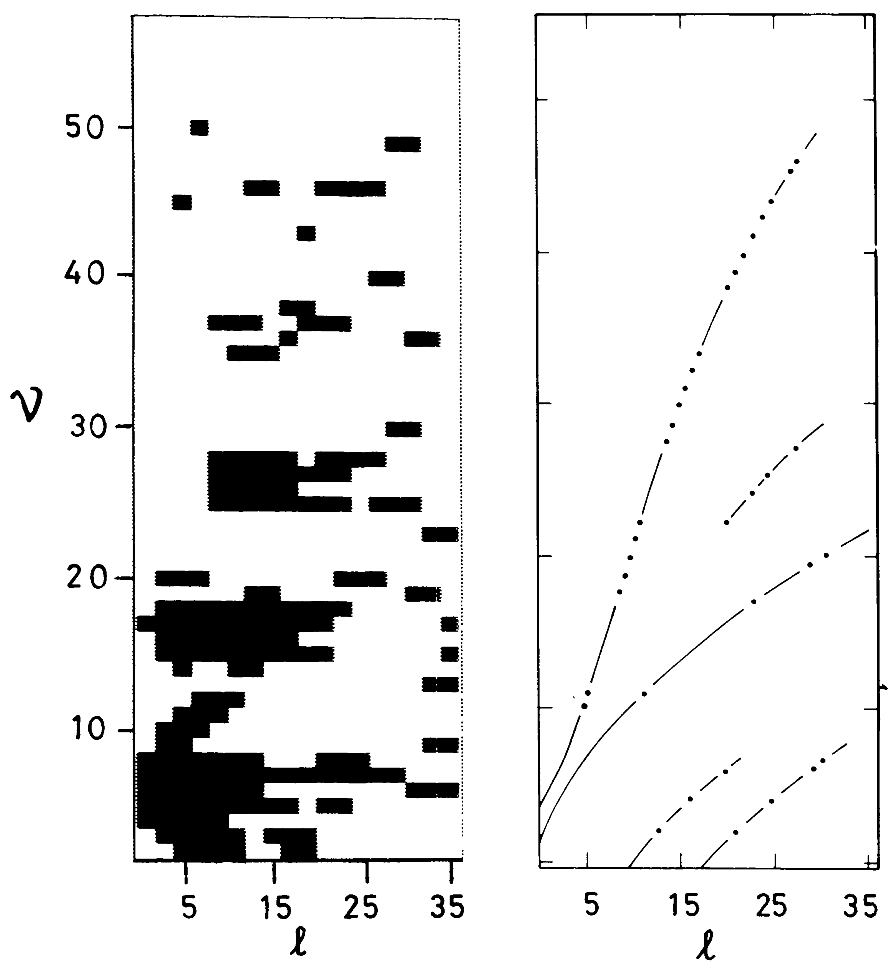

Fig. 3a.

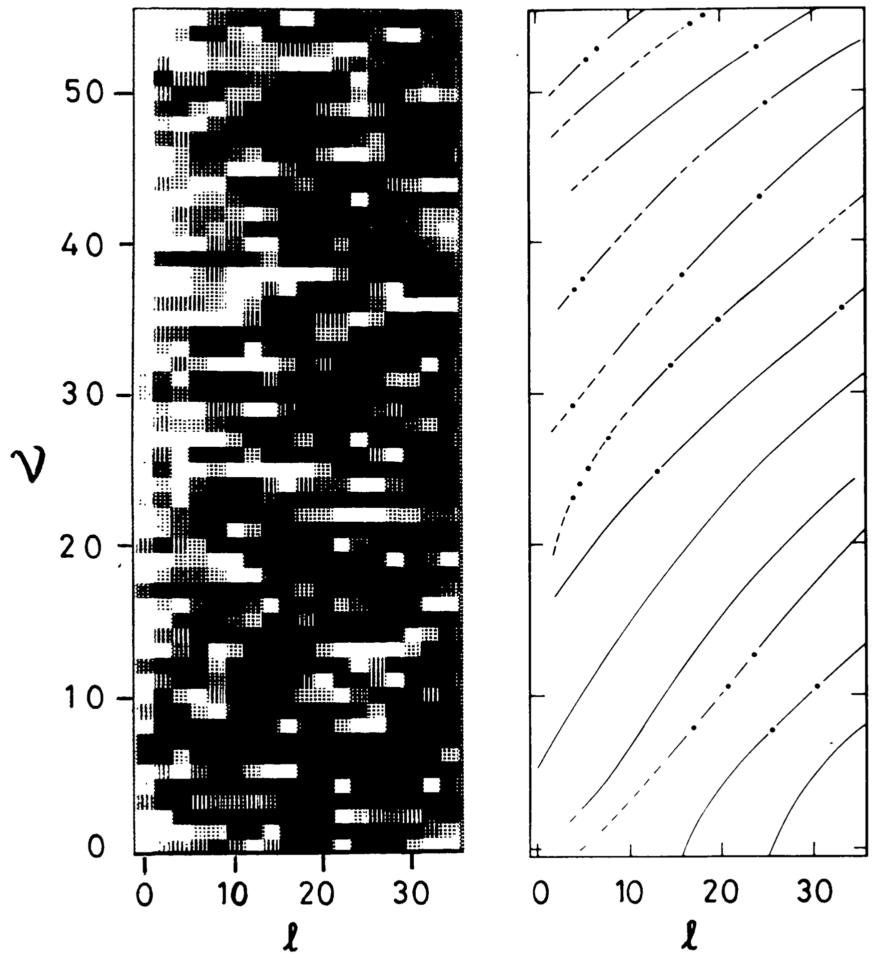

Fig. 3b.

Fig. 3. Image-processed grey-level diagrams representing the SHF power spectra corresponding to the amplitude spectra in Figures 1(a) and 1(b), respectively. The panel on the right side of each diagram shows a set of curves along which the SHF power seems to be aligned.

during 1960–1985 (Stenflo and Vogel, 1986), we recalculated the power spectrum for the even modes of the 'inferred' field during 1955–1976 with a resolution $1/32\ y^{-1}$, and made the grey-level representation of the resulting spectrum only up to $l = 14$ (Figure 4(a)). This representation indicates a distribution of power somewhat similar to, but differing in details from, the curve indicated by the magnetogram data.

The following peculiarities raise doubts about the reality of the existence of the $\nu - l$ relations indicated by the 'curves' in Figures 3(a), 3(b), and 4(a):

(i) The power distribution does not give continuous ridges along these curves, and

(ii) The curves cannot be drawn unambiguously in an objective manner. In fact some power concentrations can alternatively be considered to be lying along a set of curves with negative slopes.

4.2. Spectra obtained from two 'partly random' simulated data sets

In order to determine whether the apparent alignments of the power concentrations in the SHF spectra have any real significance, we compare these spectra with those

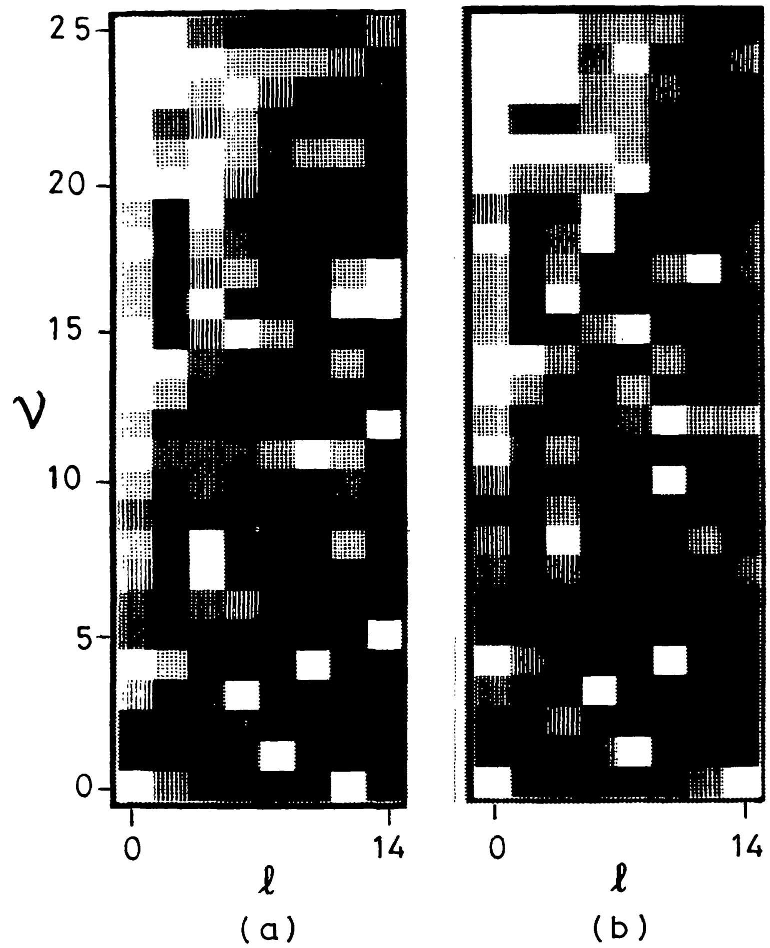

Fig. 4. (a) Grey-level diagrams representing the SHF power spectrum for the even degrees $l = 0$–14 and frequencies $\nu = 0$–25 (unit = $1/32\,y^{-1}$), obtained from the inferred magnetic field during 1955–1976. (b) Power spectrum of the 'inferred field' obtained from *simulation 'II'* during 1955–1976.

obtained from two 'partly random' simulated data sets. In both the simulated data sets, the *epochs* and the *lifetimes* of the 'sunspot groups' were assumed to be the *same* as those in the *real* data, but the latitudes of sunspot groups 'occurring' during each year and within each butterfly wing, were *redistributed* within the width of the wing in a random way. Thus, the simulation is random on scales $l \geq 13$ in *odd* parity.

In doing so, the wings given by the old and the new cycle data in each hemisphere, during the years of overlaps, were treated separately. Hence, the simulations are random on *all* scales ($l \geq 0$) in the *even* parity.

In simulation 'I' the latitudes were re-distributed with *gaussian* probability distributions, with means and standard deviations the same as those in the real data.

In simulation 'II' the redistributions were made with *uniform* distributions over the full widths defined by the yearly minimum and the maximum latitudes of the real data in the respective wings.

4.2.1. *Amplitude Spectra Given by the Simulated Data Sets*

Both the simulated data sets SI and SII yield perspective plots of SHF spectra similar to those given by the real data and, hence, those plots are not reproduced here. They are low and noisy for the even degree axisymmetric modes and show a high, smooth ridge at $\nu = \nu_* = 5\nu_0$, peaking at $l = 5, 7$ (and also low ridges along a few odd harmonics of $\nu = \nu_*$) for the odd degree axisymmetric modes. The ridges given by data sets SI and SII simulate the ridge in Figure 1(a) up to $l = 21$ and $l = 35$, respectively. This shows that the distribution of sunspot activity *within* the butterfly wings is closer to reality in the *uniform probability distribution* than in the gaussian probability distribution. For *odd* degree modes with $l \leq 11$, the similarity in the spectra of the real and the simulated data sets are a consequence of the fact that both the simulated data sets have exactly the same temporal distribution as that of the real data and also simulate the butterfly wings in the latitude time distribution.

(The differences between the results obtained from the real and the simulated data sets lie mainly in the stability of the *phases* of the various modes. The significance of these differences will be discussed in the next paper.)

4.2.2. *Grey-Level Representations of the Spectra Given by the Simulated Data Sets*

Power concentrations appear to be aligned along several curves even in the grey-level representations of the spectra obtained from the simulated data sets 'SI' and 'SII'. In Figure 5 we show the grey-level representations of the spectra given by 'SII' (the more realistic simulation). The presence of power alignments like those seen in 3(a) are expected in the region $l < 13$ of the $\nu - l$ plane for odd degree modes since on these scales and in odd parity the simulated data sets retain the systematic properties of the butterfly diagram of the real data. But the power alignments are reproduced in Figure 5 for $l \geq 0$ in even modes and also for $l \geq 13$ in odd modes, on which scales the latitudes are randomly distributed in 'SI' and 'SII'. Hence, the alignments in Figure 3 cannot be taken as evidence for any physical relation between the ν and l of the modes in the real data.

This rejection, based on reproduction by the simulated data set, is not applicable to the 'wisp' extending from ($l = 3$, $\nu = 8$) to ($l = 11$, $\nu = 11$) in Figure 3(a), which is reproduced in Figure 5(a), since it is in the non-random ($l < 13$) domain of scales. Yet it cannot be considered as representing a $\nu - l$ relation. For if it were due to real oscillations, similar wisps would be found at $\nu = 3\nu_*$, $5\nu_*$, etc., irrespective of whether the power in the odd harmonics is due to mathematical nonlinearity or resonance excitation.

For comparison with the results obtained from the magnetogram data, we have computed the SHF spectrum of the *even* modes in a simulation 'II' of the data $B_{\rm inf}(\theta, \phi, t)$ during the interval 1960–1976, with a frequency resolution $\sim 1/32\ y^{-1}$. The grey level representation of this spectrum is given in Figure 4(b). This contains concentrations apparently aligned in a way somewhat similar to that in Figure 4(a). Hence, the alignment in Figure 4(a) also cannot be considered as significant.

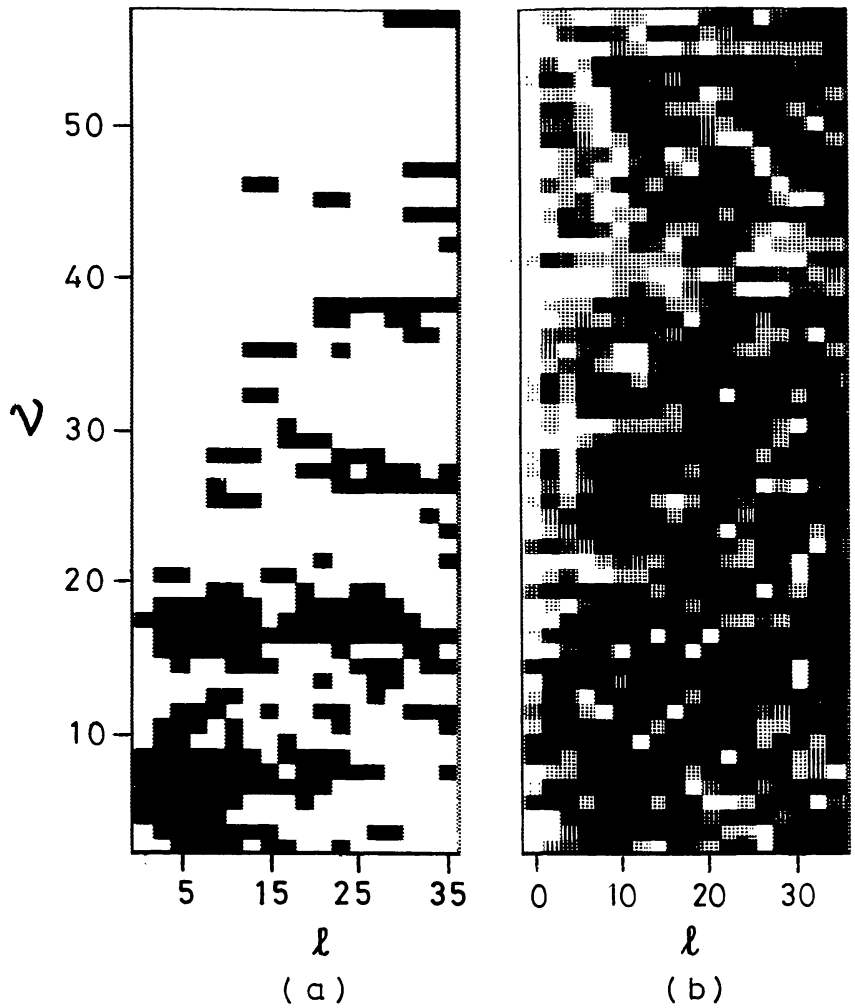

Fig. 5. Grey-level representations of the SHF power spectra of (a) odd and (b) even degree modes in *simulation II* of the inferred field during 1874–1976.

We conclude that the 'curves' apparently 'passing through' the power concentrations in the odd or even degree axisymmetric SHF modes in the magnetic field inferred from the sunspot data need not represent any real relations between the harmonic degrees and the frequencies of the modes in the data.

5. Conclusions and Discussion

The refined analysis of the Sun's magnetic field 'inferred' from the sunspot data, which is presented here, confirms the earlier result that the sunspot data can be used to study, even quantitatively, the global behaviour of the solar magnetic field during several cycles before the beginning of the regular magnetogram observations, at least on large scales.

The most important conclusion of the analysis is that there is no convincing evidence for the existence of any relation between the frequency (ν) and the degree (l) of either odd or even degree axisymmetric modes, whatever be the physical nature of the modes.

The narrow band widths of the ridges at ν_*, $3\nu_*$, $5\nu_*$, etc. in Figure 1(a) provide the following clues for the theoretical modelling. One possibility is that the internal thermal and magnetic field of the Sun are so structured that the frequencies of all the admissible modes lie in band widths $\sim \nu_0$ around ν_*, $3\nu_*$, $5\nu_*$, ..., etc. The other, more straightforward, interpretation of Figure 1(a) is that the basic oscillations may be 'forced' (e.g., through boundary conditions imposed on the 'dynamo' by some 'clock' in the deep solar interior as suggested by Dicke, 1977). The approximate constancy of the band widths of the 'ridges' at ν_*, $3\nu_*$, etc. in Figure 1(a) suggests that the band width of the 'forcing frequency' is much less than ν_0, i.e., $\ll 1/107\ y^{-1}$.

The difference between the noise levels in Figures 1(a) and 2 shows that the lifespan of a sunspot group yields a smoother measure of the 'inferred field intensity', and hence a better measure of the magnetic flux responsible for producing the spot group.

For $l \leq 13$ and all ν, the SHF spectra of odd degree modes in the real and the simulated data sets are similar because the time 'epochs' of 'spot groups' in the three data sets are the same and the simulated data sets are generated using the real butterfly diagrams. The differences between the real and the simulated data sets would lie in the distribution of activity *within* the wings of the butterflies. Simulation II gives a better description of this distribution than simulation I. Yet, there are significant differences between the results obtained from the real distribution and from simulation II. These will be discussed in the next paper.

The sunspot butterfly diagrams, migrations of latitude zones of prominences, etc., have long since suggested that the *basic mechanism* of the solar magnetic cycle is a *global* process. The SHF analysis is based on a tacit belief that the 'global process' can be described in terms of some physically real global 'oscillations' or 'waves' represented by terms, or more probably *groups* of terms, in the SHF analysis. This belief was somewhat strengthened by the 'phase stability' of the major ($l \geq 13$) SHF modes (e.g., Gokhale, Javaraiah, and Hiremath, 1990), as implied by the regularity of the butterfly diagrams. Substantial evidence for the magnetic cycle to be made up of such global oscillations comes from the phase stability of even the higher degree modes, and the predictability of the field behaviour in high latitudes as shown in the next paper. Theoretical modelling will be needed to determine the physical nature of such global oscillations. These could either represent oscillatory solutions of the dynamo equations, or may themselves be dynamical (e.g., MHD, torsional, etc.) oscillations of the whole Sun.

In the later case it is important to note that the odd parity of the 'forced' oscillations would be consistent with torsional MHD oscillations of *even* parity in the presence of a zero order poloidal field of dipole-like parity. The power peak at $l = 5$–7 would correspond to dominance of $l = 4$–8 in the torsion. It is significant in this context that the torsional oscillations detected by LaBonte and Howard (1982) have latitude variations similar to those of Legendre polynomials of $\cos\theta$ for l in this range.

Acknowledgement

We thank Dr H. Balthasar for providing the magnetic tape of the Greenwich sunspot data.

References

Bracewell, B. N.: 1988, *Monthly Notices Roy. Astron. Soc.* **230**, 535.
Dicke, R. H.: 1977, *Astrophys. J.* **218**, 547.
Gokhale, M. H. and Javaraiah, J.: 1990a, *Monthly Notices Roy. Astron. Soc.* **243**, 241.
Gokhale, M. H. and Javaraiah, J.: 1990b, in E. R. Priest and V. Krishan (eds.), 'Basic Plasma Processes on the Sun', *IAU Symp.* **142**, 119.
Gokhale, M. H., Javaraiah, J., and Hiremath, K. M.: 1990, in J. O. Stenflo (ed.), 'Solar Photosphere, Structure, Convection and Magnetic Fields', *IAU Symp.* **138**, 375.
LaBonte, B. J. and Howard, R.: 1982, *Solar Phys.* **75**, 161.
Stenflo, J.: 1988, *Astrophys. Space Sci.* **144**, 321.
Stenflo, J. and Vogel, M.: 1986, *Nature* **319**, 285.